Molecular Crystals and Liquid Crystals Science and Technology. Section A. Molecular Crystals and Liquid Crystals
Publication details, including instructions for authors and subscription information:
http://www.tandfonline.com/loi/gmcl19

Synthesis and Characterization of Ferroelectric and Antiferroelectric Liquid Crystals Derived from (2S)-2-(6-Hydroxy-2-Naphthyl) Propionic Acid

S.-L. Wu [a], D.-G. Chen [a], S.-J. Chen [a], C.-Y. Wang [b], J.-T. Shy [b] & G.-H. Hsiue [c]

[a] Department of Chemical Engineering, Tatung Institute of Technology, Taipei, 10451, Taiwan ROC

[b] Department of Physics, National Tsing Hua University, Hsinchu, 30043, Taiwan ROC

[c] Department of Chemical Engineering, National Tsing Hua university, Hsinchu, 30043, Taiwan ROC

Version of record first published: 23 Sep 2006.

To cite this article: S.-L. Wu , D.-G. Chen , S.-J. Chen , C.-Y. Wang , J.-T. Shy & G.-H. Hsiue (1995): Synthesis and Characterization of Ferroelectric and Antiferroelectric Liquid Crystals Derived from (2S)-2-(6-Hydroxy-2-Naphthyl) Propionic Acid, Molecular Crystals and Liquid Crystals Science and Technology. Section A. Molecular Crystals and Liquid Crystals, 264:1, 39-50

To link to this article: http://dx.doi.org/10.1080/10587259508037300

Mol. Cryst. Liq. Cryst., 1995, Vol. 264, pp. 39–50
Reprints available directly from the publisher
Photocopying permitted by license only

Synthesis and Characterization of Ferroelectric and Antiferroelectric Liquid Crystals Derived from (2S)-2-(6-Hydroxy-2-Naphthyl)Propionic Acid

S.-L. WU, D.-G. CHEN and S.-J. CHEN

Department of Chemical Engineering, Tatung Institute of Technology, Taipei 10451, Taiwan ROC

C.-Y. WANG and J.-T. SHY

Department of Physics, National Tsing Hua University, Hsinchu 30043, Taiwan ROC

and

G.-H. HSIUE

Department of Chemical Engineering, National Tsing Hua University, Hsinchu 30043, Taiwan ROC

(Received December 9, 1993; in final form June 27, 1994)

A new series of chiral materials, hexyl(2s)-2-(6-(-4-(4'-alkoxyphenyl)benzoyloxy)-2'-naphthyl) propionates (HmPBNP; $m = 6$–18) had been prepared and their liquid crystalline properties were investigated as a function of alkyl chain length. These chiral materials exhibited novel ferroelectric S_c^* and antiferroelectric Sc_A^* phases and a propensity to the formation of the Sc_A^* phase was found at longer alkyl chain lengths ($m = 10, 12$–18). An odd-even effect of the threshold voltage as a function of alkyl chain length for compounds HmPBNP ($m = 12$–16) possessing antiferroelectricity was observed. Spontaneous polarization and transverse dipole moment were also measured and are discussed in terms of the elongated alkyl chain length.

Keywords: Ferroelectric liquid crystal, antiferroelectric liquid crystal, spontaneous polarization

INTRODUCTION

The antiferroelectric Sc_A^* phase[1] has become of great interest recently since it possesses a tristable switching property[1,2] with application potential for the fast-switching electro-optical devices.[3–5] However, since only a few materials possessing Sc_A^* phase have been prepared and reported,[2,6–13] the details concerning the relationship between molecular structure and the appearance of Sc_A^* phase have not yet been fully established. Thus, the design and synthesis of new materials have become one of the major research subjects for the synthetic scientists in order to bring about a better understanding of this issue.

Nishiyama and Goodby[11] pointed out that most materials exhibiting Sc_A^* phase have molecular structures where a chiral centre is located in a position that is relatively closed to the central rigid core of the molecule. On this basis, the derivatives of (2S)-2-(6-hydroxy-2-naphthyl)propionic acid, where the chiral centre located in the vicinity of the rigid core should be candidates for study. The general molecular structure for the homologous series of the chiral materials, hexyl(2S)-2-(6-(4-(4′-alkoxyphenyl)benzoyloxy)-2′-naphthyl) propionates (HmPBNP) is given below:

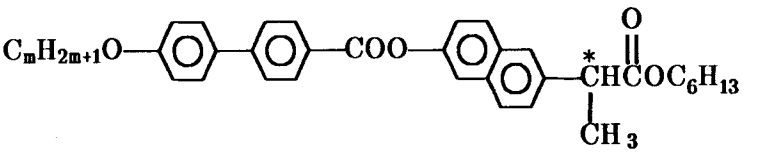

The liquid-crystalline mesophases and some physical properties are reported and discussed in terms of the alkyl chain length.

EXPERIMENTAL

The chiral starting material for the synthesis of the compounds HmPBNP is (2S)-2-(6-methoxy-2-naphthyl) propionic acid, was purchased from Tokyo Chemical Industry (TCI) Co. Ltd., with optical purity greater than 99% ee. The synthetic procedures were carried out according to scheme 1. The acid **1** was esterified with 1-hexanol in the presence of *N*,*N*′-dicyclohexylcarbodiimide (DCC) and 4-*N*,*N*-dimethylamino-pyridine (DMAP) to produce the ester, hexyl(2S)-2-(6-methoxy-2-naphthyl) propionate **2**. The methoxy group of this ester was demethylated by treatment with BBr_3, and the resulting hydroxy group of hexyl(2S)-2-(6-hydroxy-2-naphthyl) propionate **3** was subsequently esterified with a selection of 4-(4′-alkoxyphenyl)benzoic acids **5** using DCC and DMAP to produce the target compounds. The detailed synthetic procedures will be reported elsewhere.[14]

All intermediates and final products were preliminarily isolated by column chromatography over silica gel (70–230 mesh) using dichloromethane as eluent, and further purified by recrystallization from hexane or absolute ethanol. The chemical structures for all materials prepared were analyzed by nuclear magnetic resonance (NMR) spectroscopy using a Buker WP100SY FT-NMR spectrometer. The purity of the final compounds were checked by thin-layer chromatography. Further confirmation for the purity was done by elemental analysis using a Perkin-Elmer 2400 instrument. Specific rotations were measured in dichloromethane using A JASCO DIP-360 digital polarimeter. Transition temperatures and enthalpies of the transition were determined by differential scanning calorimetry (DSC) using a DuPont DSC-910 calorimeter at a rate of $2^{\circ}C\,min^{-1}$. Mesophases are identified by observation of the textures using a Nikon Microphot-FXA optical microscope under crossed polarizers

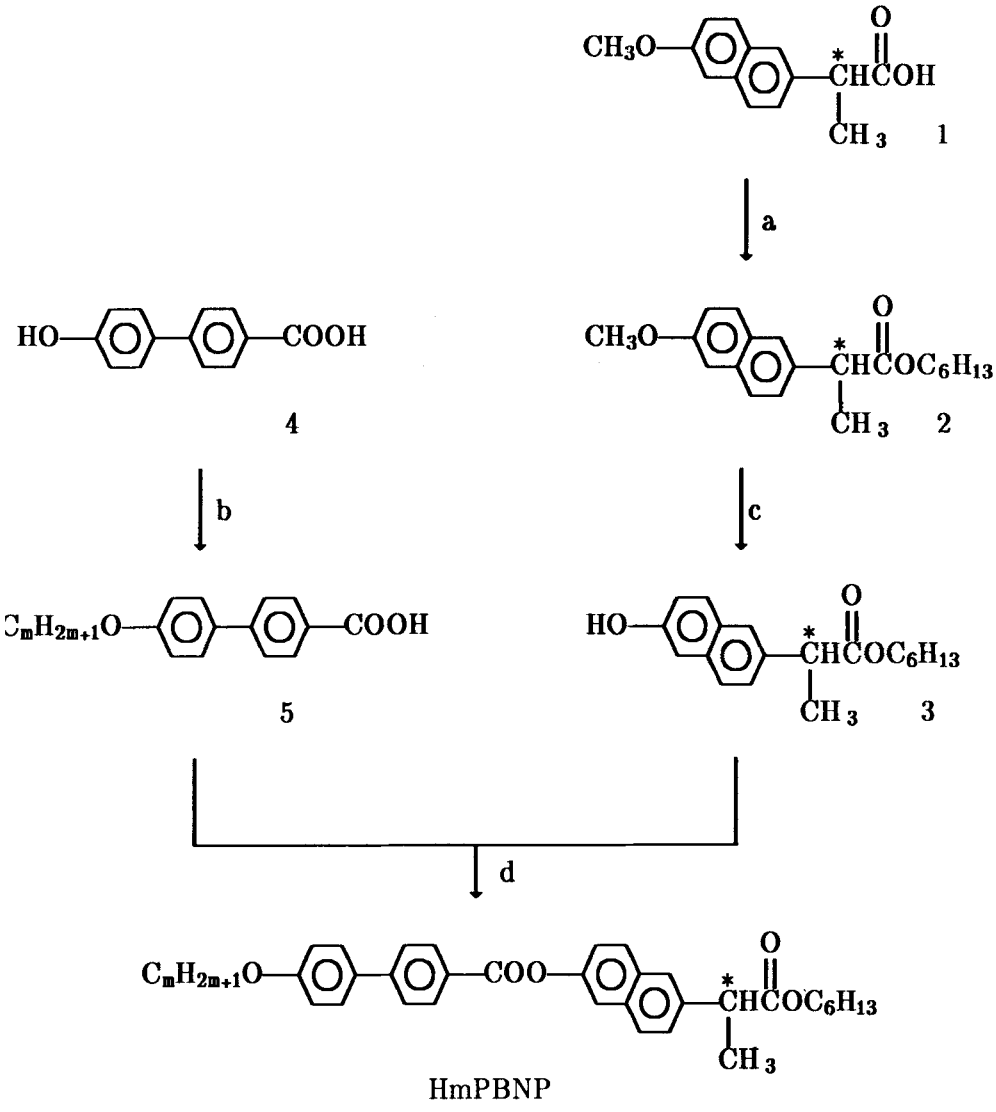

SCHEME 1 a. $C_6H_{13}OH$, DCC, DMAP,CH_2Cl_2; b. $C_mH_{2m+1}Br$, KOH; c. BBr_3, CH_2Cl_2; d. DCC, DMAP, THF.

with a Mettler FP82-HT hot stage connected to a Mettler FP80-HT heat controller. Sample cells of each liquid crystal were fabricated by ITO glasses coated with unidirectionally buffed polyimide film. The cell gap was 5 μm and the electrically conducting area was 0.25 cm^2. The magnitudes of the spontaneous polarization were measured by the triangular wave method.[11]

RESULTS AND DISCUSSION

Synthesis

The NMR analysis for the main product of each synthetic procedure showed that the characteristic singlet of the methoxy group for hexyl (2S)-2-(6-methoxy-2-naphthyl) propionate appeared at $\delta = 3.9$ ppm ($CDCl_3$). This peak disappears after demethylation, and the resulting hydroxy proton for hexyl (2S)-2-(6-hydroxy-2-naphthyl) propionate found down field at $\delta = 5.2$ ppm ($CDCl_3$). This hydroxy proton peak is lost upon further esterification to produce the final product.

The results of elemental analysis for HmPBNP are listed in Table 1. The percentage errors for the carbon and hydrogen contents were less than 2% as compared to the calculated results.

The optical purity of intermediates and products in each synthetic step was not examined. However, since the esterification using DCC and DMAP,[15] and the demethylation using boron tribromide[16] have been reported to be free from racemization, it can be expected that compounds HmPBNP should possess high optical purity. The specific rotations for HmPBNP measured in dichloromethane are also summarized in Table 1.

TABLE I

Results of Elemental analysis and specific rotation $[\alpha]_D$ for compounds HmPBNP

Compounds	Elemental analysis		$[\alpha]_D^{25.6}$(conc.)*
HmPBNP	C%	H%	
H6PBNP	Calc. 78.59	7.64	+15.36(0.652)
	Found 78.69	7.66	
H7PBNP	Calc. 78.76	7.80	+15.07(0.650)
	Found 78.77	7.83	
H8PBNP	Calc. 78.95	7.89	+14.44(0.640)
	Found 78.66	7.94	
H9PBNP	Calc. 79.06	8.09	+13.87(0.620)
	Found 79.20	8.13	
H10PBNP	Calc. 79.28	8.18	+14.18(0.642)
	Found 79.09	8.22	
H11PBNP	Calc. 79.35	8.36	+12.30(0.634)
	Found 79.33	8.44	
H12PBNP	Calc. 79.52	8.44	+14.66(0.645)
	Found 79.64	8.43	
H13PBNP	Calc. 79.61	8.61	+14.77(0.642)
	Found 79.60	8.67	
H14PBNP	Calc. 79.73	8.73	+10.42(0.650)
	Found 79.71	8.84	
H15PBNP	Calc. 79.88	8.80	+10.36(0.654)
	Found 80.27	8.85	
H16PBNP	Calc. 79.96	8.95	+10.04(0.624)
	Found 79.30	8.99	
H18PBNP	Calc. 80.17	9.15	+9.36(0.623)
	Found 80.15	9.21	

* Concentration in g/100 cm^3

Transition Temperatures and Mesophases

The mesophase transition temperatures for HmPBNP were determined by DSC in conjunction with optical microscopy. Mesophase identification was carried out principally by the textures observed by optical microscopy. Ferroelectric Sc* and antiferroelectric Sc_A* phases were further characterized by other electro-optical methods.[17]

Representative DSC thermograms for compounds HmPBNP ($m = 7$, 10 and 13) are depicted in Figure 1 in the cooling process. Figure 1 (a) refers to the cooling trace of H7PBNP indicating that, as the temperature is lowered from the isotropic liquid (Iso), the phase transitions occur initially from Iso to N* phase at 143.8°C, and subsequently to the S_A phase at 143°C. A slightly different DSC pattern is shown in Figure 1 (b) for H10PBNP. It shows in addition to an Iso-N* transition at 136.1°C and a N*-S_A transition at 135.2°C, there is a small jut in the baseline at 108°C corresponding to a S_A-Sc* transition based on the change in optical microscopic texture. A non-

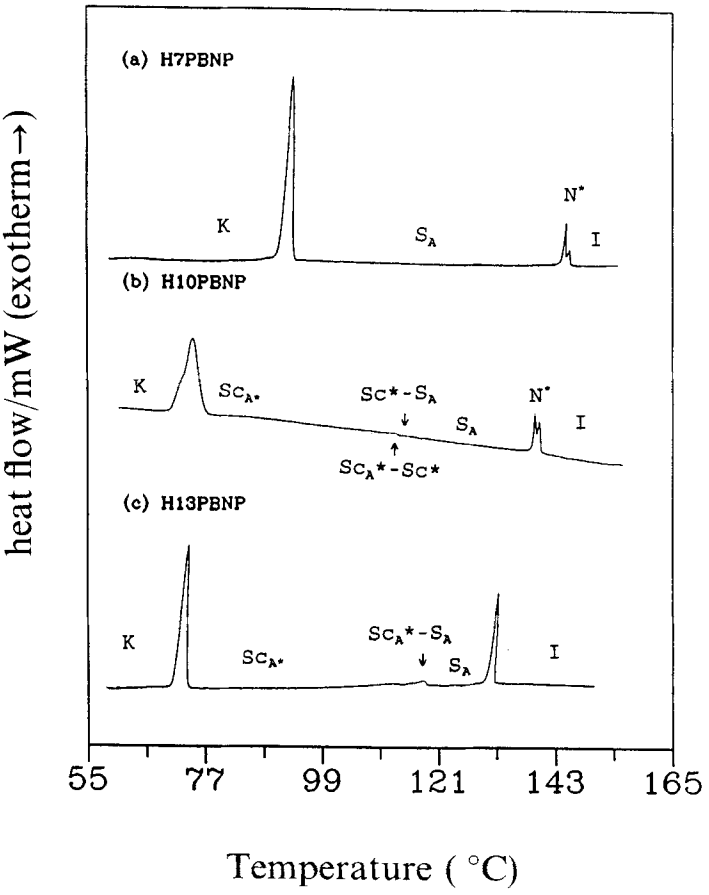

FIGURE 1 Representative DSC thermograms for compounds HmPBNP ($m = 7$, 10, and 13) in the cooling process (cooling rate 2°C min^{-1}).

observable phase transition along the DSC trace occured at 107.6°C was found and could be identified as a Sc*-Sc_A* transition. This compound exhibits two additional novel phases: ferroelectric Sc* and antiferroelectric Sc_A* phases. Figure 1 (c) refers to the DSC trace for H13PBNP. There is only a significant Iso-S_A transition at 130.3°C. A small jut in the baseline at 117.6°C was identified as a S_A-Sc_A* transition. This compound has no ferroelectric Sc* phase but a novel antiferroelectric Sc_A* phase existed. The enthalpies for the I-N* and N*-S_A transitions are large, thus, these transitions are first order. The enthalpies for the S_A-Sc*, Sc*-Sc_A* and $S_A - Sc_A$* transitions, however, are much smaller or even non-detectable, thus, these transitions are second order in nature.

The mesomorphic phases, transition temperatures and enthalpies of the phase changes are summarized in Table 2. A phase diagram as the function of the alkyl chain length, *m*, is plotted in Figure 2. It shows that as m increases, the clearing-point transition falls. The N* phase is formed for m ranging from 7 to 10, but the phase temperature ranges are rather narrow. The N*-S_A transition temperatures also decrease when the vlaues of *m* were increased. All compounds exhibited a S_A phase. Ferroelectric Sc* phase appeared when *m* was greater than 7. Interestingly, the S_A-Sc* transition temperatures increased in parallel to *m* up to 11 and then levelled off as *m* was increased further. These results in conjunction with the fall in the Iso-S_A transition temperature with increasing *m* values, results in a decline in the thermal stabilities of S_A phase with increasing alkyl chain length. The antiferroelectric Sc_A* phase appeared when *m* was greater than 9. It is worthy of note that, with the exception of $m = 11$, the

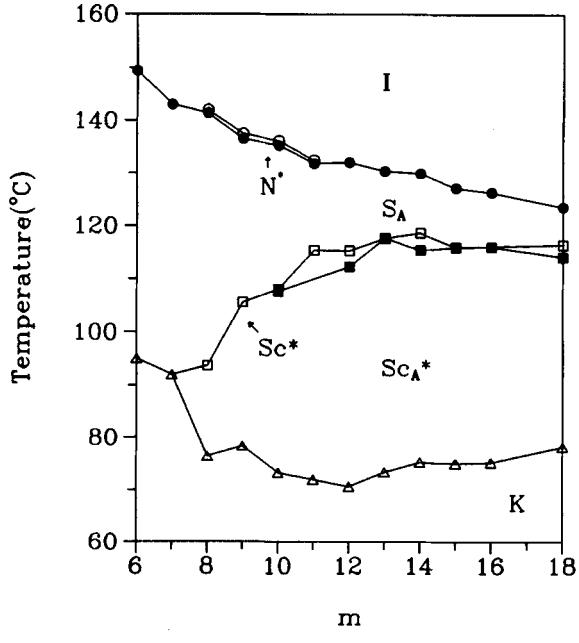

FIGURE 2 A plot of transition temperatures as function of alkyl chain length for HmPBNP. O, I—N*; ●, N* or I—S_A; □, S_A-Sc*; ■, S_A or Sc*-Sc_A*; Δ, S_A or Sc* or Sc_A*-K.

TABLE II

Transition temperatures and enthalpy of phase changes for the compounds HmPBNP

Compounds	Iso-N*		Iso or N*-S_A		S_A – Sc*		S_A or Sc*-Sc_A*		S_A or Sc* or Sc_A*-K	
HmPBNP	T	ΔH[a]	T	ΔH	T	ΔH	T	ΔH	T	ΔH
H6PBNP	–	–	149.4	5.93	–	–	–	–	95.1	40.88
H7PBNP	143.8	0.81	143.0	2.73	–	–	–	–	92.0	45.88
H8PBNP	142.0	1.12	141.1	2.40	93.7	[b]	–	–	76.9	76.13
H9PBNP	137.5	1.10	136.5	1.55	105.6	[b]	–	–	78.3	36.46
H10PBNP	136.1	1.57	135.2	1.74	108.0	0.35	107.6	[b]	73.2	46.75
H11PBNP	132.4	0.69	131.8	0.70	115.4	0.23	–	–	71.9	33.26
H12PBNP	–	–	132.0	4.27	115.3	0.32	112.3	[b]	70.6	26.94
H13PBNP	–	–	130.3	4.95	–	–	117.6	[b]	73.3	29.52
H14PBNP	–	–	129.9	5.70	118.6	0.02	115.4	[b]	75.2	38.14
H15PBNP	–	–	127.1	2.58	–	–	115.9	[b]	74.9	21.85
H16PBNP	–	–	126.3	5.60	–	–	116.0	[b]	75.1	51.89
H18PBNP	–	–	123.5	5.48	116.4	[b]	114.1	[b]	78.2	61.46

[a] Temperature unit is °C and enthalpy unit is J/g.
[b] Enthalpy is too small to be measured.

occurrence of Sc_A^* phase suppresses the stability of Sc* phase. Moreover, in the cases of $m = 13$, 15 and 16, the presence of Sc_A^* phase even eclipses the S_A-Sc* transition. Surprising as it may seem, these results strongly suggest that the elongation of the alkyl chain favours the formation of Sc_A^* phase rather than that of Sc* phase in this series of compounds. Figure 2 also indicates that the existence of the Sc* phase or Sc_A^* phase causes a decrease of the temperatures for crystalline formation. Consequently, the thermal stability of Sc* phase is increased as m varies from 8 to 9, and that of Sc_A^* phase becomes wider as the alkyl chain is further lengthened.

Physical Properties of Sc* and Sc_A^* Phases

The apparent tilt angles of compounds HmPBNP as function of the applied DC voltages were investigated using 5 μm cells for the characterization of the existing Sc_A^* phase. A typical example, obtained from the experimental result of H12PBNP at 110.3 °C, is shown in Figure 3. It is noted that there exists a double hysteresis loop with sharp threshold voltages for both increasing and decreasing applied voltages, corresponding to the switching between antiferroelectric and ferroelectric states.

In order to correlate the structure-property relationship for HmPBNP, the transition temperature (Tc) for Sc*-Sc_A^* and S_A-Sc_A^* phases were investigated by the triangular wave method and the results are summarized in Table 3. The threshold

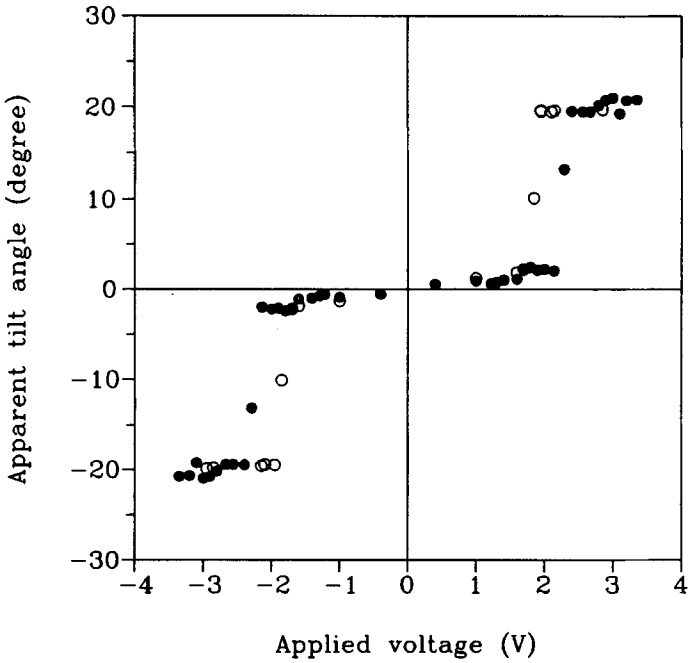

FIGURE 3 Hysteresis in an apparent tilt angle as a function of an applied DC voltage for compound H12PBNP. ●, Increasing voltage; ○, Decreasing voltage.

TABLE III

Physical properties of compounds HmPBNP

Compounds HmPBNP	Tc[a] (°C)	Ps[b] nC/cm^2	tilt angle θ^b degree	Po[c] nC/cm^2	sign of Ps
H8PBNP	93.7	38.56	24.4	93.37	+
H9PBNP	103.6	27.88	21.6	75.74	+
H10PBNP	106.8	24.88	18.3	79.24	+
H11PBNP	113.2	20.46	17.2	69.19	+
H12PBNP	113.5	40.96	21.4	112.26	+
H13PBNP	115.5	36.66	20.1	106.68	+
H14PBNP	118.6	37.28	18.8	115.68	+
H15PBNP	111.3	28.95	17.9	94.19	+
H16PBNP	111.6	39.31	21.0	109.69	+
H18PBNP	115.4	22.78	17.6	75.34	+

[a] The transition temperature *Tc* which represent S_A-Sc* transition temperature or S_A-Sc$_A$* transition temperature was determined by triangular wave method in 5 μm thickness cell.

[b] The physical properties of compounds HmPBNP were measured at 5 °C below the *Tc*.

[c] The value of *Po* is the ratio of *Ps*/sin θ.

voltages for HmPBNP measured at 5°C below *Tc* were plotted as function of *m* as presented in Figure 4. It is found that there is an odd-even effect of threshold voltages in the consecutive elongation of alkyl chain length ($m = 12$–16) for both increasing and decreasing applied voltages. This phenomenon is presumably attributed to the effect of

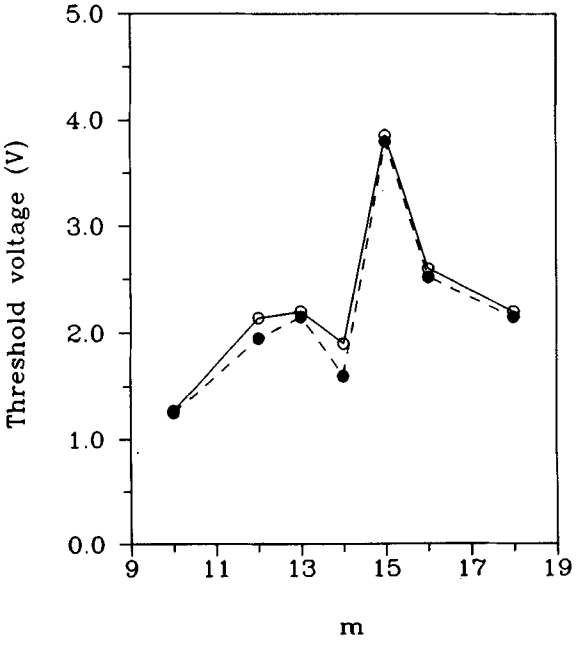

FIGURE 4 The threshold voltages as function of alkyl chain length in the antiferroelectric phase for compounds HmPBNP. ○, antiferroelectric-ferroelectric state; ●, ferroelectric-antiferroelectric state.

the elongated terminal methyl group on- or off-axis along the molecular axis; however, the real cause is not clear at present. Remarkably enhanced threshold voltages are observed in compound H15PBNP, however, the occurrence of this anomaly is also not clear at present. Figure 4 also strongly suggests that the width of the hysteresis loops are critically dependent on the nature of alkyl chain length.

The magnitudes of the spontaneous polarization (*Ps*) were measured by the triangular wave method. Typical examples of compounds H9PBNP, H12PBNP and H13PBNP for the *Ps* values as the function of temperature are shown in Figure 5. It is seen that *Ps* values gradually decrease as the temperature increases. The nature of the *Ps* value with respect to temperature seems not to be influenced by the existence of Sc* phase as in compound H9PBNP, Sc_A* phase in H13PBNP, or the coexistence of Sc* and Sc_A* phases in H12PBNP, although the switching for Sc* phase is proposed as a transient between two stable ferroelectric states, whereas that for Sc_A* phase as a transient from one induced-ferroelectric state to another ferroelectric state.[12] The *Ps* values and corresponding optical tilt angles (θ) measured at 5°C below S_A-Sc* or S_A-Sc_A* transition temperature for all materials are also listed in Table 3. The results of *Ps* and θ values show no correlation with the alkyl chain length. Thus, the transverse dipole moment (P_o) for all materials is calculated for comparison. The *Po* and *Ps* values plotted as a function of *m* are shown in Figure 6. An odd-even effect of transverse dipole moment with respect to the alkyl chain length is observed. This effect is also presumably attributed

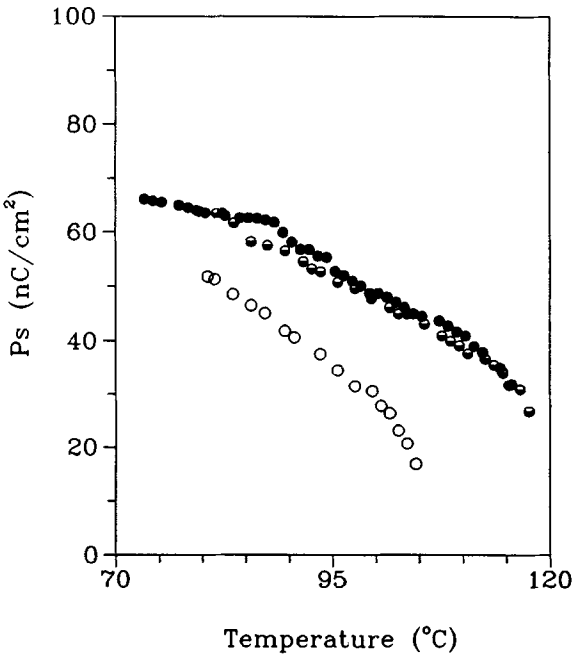

FIGURE 5 The magnitude of spontaneous polarization *Ps* as a function of temperature in ferroelectric and antiferroelectric phases for compounds HmPBNP. ○, $m = 9$; ●, $m = 12$; ●, $m = 13$.

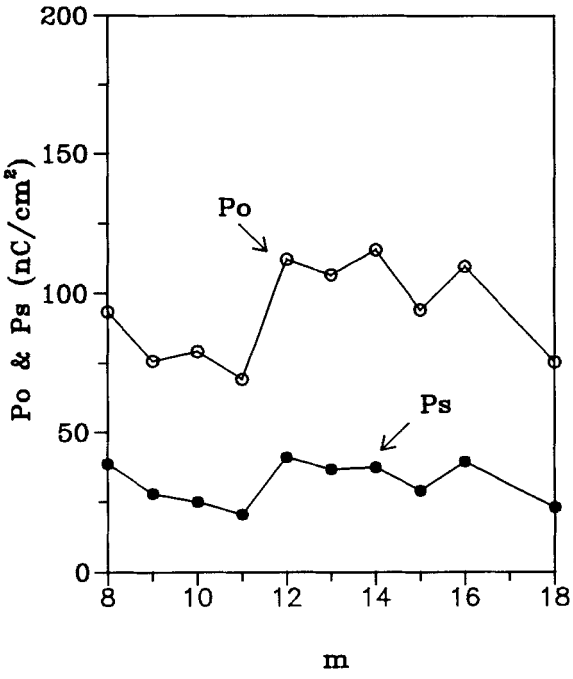

FIGURE 6 Transverse dipole moments P_0 (○) and spontaneous polarization Ps (●) as function of elongated alkyl chain length for compounds HmPBNP measured at 5°C below the S_A-Sc* or S_A-Sc_A* transition temperature.

to the effect of the elongated terminal methyl group along the molecular long axis.[18] A positive sign of Ps for all compounds measured by field reversal method[19] was obtained.

CONCLUSION

The chiral materials HmPBNP derived from (2S)-2-(6-hydroxy-2-naphthyl) propionic acid in which the chiral centre is located in the vicinity of the rigid core have been found to show an antiferroelectric Sc_A* phase. A propensity for the formation of Sc_A* phase has been found at longer alkyl chain length. The thermal stability of the Sc_A* phase is not significantly influenced by the elongated alkyl chain length. An odd-even effect is observed in the threshold DC voltage of Sc_A* phase and the transverse dipole moment as a function of the alkyl chain length.

Acknowledgements

This work was supported by the National Science Council under Grand No. NSC-82-0511-E007-01.

References

1. A. D. L. Chandani, Y. Ouchi and H. Takezoe, *Jpn. J. Appl. Phys.*, **28**, L1261 (1989).
2. A. D. L. Chandain, T. Hagiwarn, Y. Suzuki, Y. Ouchi, H. Takezoe and A. Fukuda, *Jpn. J. Appl. Phys.*, **27**, L729 (1988).
3. N. Yamamoto, Y. Yamada, N. Koshobu, K. Mori, K. Nakamda, H. Orihara, Y. Ishibashi, Y. Suzuki and I. Kawamur, *Jpn. J. Appl. Phys.*, **31**, 3186 (1992).
4. T. Moriyama, J. Kajita, Y. Takanishi, K. Ishikawa, H. Takezoe and F. Fukuda, *Jpn. J. Appl. Phys.*, **32**, 589(1993).
5. T. Orama, T. Masuda, S. Hamada, S. Takahashi, S. Kurita, I. Kawamura and T. Hagiwara, *Jpn. J. Appl. Phys.*, **32**, L668 (1993).
6. I. Wishiyama, A. Yoshizawa, M. Fukumasa and T. Hirai, *Jpn. J. Appl. Phys.*, **28**, L2248 (1989).
7. Y. Suzuki, T. Hagiwara and I. Kawamura, *Liq. Cryst.*, **6**, 167 (1989).
8. S. Inui, S. Kawano, M. Saito, H. Iwane, K. Hiraoka, Y. Ouchi, H. Takezoe and F. Fukuda, *Jpn. J. Appl. Phys.*, **29**, L987 (1990).
9. T. Isozaki, Y. Suzuki, I. Kawamura, K. Mori, N. Yamamoto, Y. Yamada, H. Orihara and Y. Ishibashi, *Jpn. J. Appl. Phys.*, **30**, L1573 (1991).
10. J. W. Goodby, J. S. Patel and E. Chin, *J. Mater. Chem.*, **2**, 197 (1992).
11. I. Nishiyama and J. W. Goodby, *J. Mater. Chem.*, **2**, 1015 (1992).
12. I. Nishiyama and J. W. Goodby, *J. Mater. Chem.*, **3**, 149 (1993).
13. J. W. Goodby, I. Nishiyama, A. J. Slanely, C. J. Booth and K. J. Toyne, *Liq. Crysts.*, **14**, 370 (1993).
14. S. L. Wu, D. G. Chen, W. J. Hsieh, L. J. Yu and J. J. Liang, *Mol. Cryst. Liq. Cryst* -in press (LC-AG-23).
15. G. Stork and S. D. Rychnovsky, *J. Am. Chem. Sco.*, **109**, 1565 (1987).
16. T. Kusumoto, T. Ueda, T. Hiyama, S. Takehara, T. Shoji, M. Osawa, T. Kuriyama and T. Fujisawa, *Chem. Lett.*, 523 (1990).
17. Y. Takanishi, H. Takezoe, A. Fukuda, H. Komura and J. Watanabe, *J. Mater. Chem.*, **2**, 71 (1992).
18. J. W. Goodby, J. S. Patel and E. Chin, *J. Phys. Chem. Lett.*, **91**, 5151 (1987).
19. J. W. Goodby, E. Chin, T. M. Leslie, J. M. Geary and J. S. Patel, *J. Am. Chem. Soc.*, **108**, 4729 (1986).